Enhanced Dye-Sensitized Photoconversion Efficiency via Reversible Production of UV-Induced Surface States in Nanoporous TiO_2

Brian A. Gregg,* Si-Guang Chen, and Suzanne Ferrere*

National Renewable Energy Laboratory, 1617 Cole Blvd., Golden, Colorado 80401

Received: September 5, 2002; In Final Form: January 28, 2003

Brief UV illumination of dye-sensitized solar cells can result in a remarkable increase in their photoconversion efficiency (Ferrere, S; Gregg, B. A. *J. Phys. Chem. B* **2001**, *105*, 7602). Further investigation of this phenomenon reveals that a major effect of UV illumination is to reversibly create a high concentration of photoactive surface states continuously distributed below the conduction bandedge in the nanoporous TiO_2 films. The ability to create, and then eliminate, surface states allows, for the first time, a clear assessment of the influence of these states on the dye-sensitization process. Positive conduction bandedge (mobility edge) shifts apparently also result from UV illumination, and the difficulties in quantifying such shifts in functioning cells are discussed. We conclude that the major cause of the increased efficiency is the photoproduction of surface states that may improve photoinjection and carrier transport while possibly slowing the recombination rate. The creation of these surface states is strongly inhibited by the presence in the electrolyte solution of the Li^+ ion, which is known to specifically adsorb to TiO_2 surfaces. We present an in-depth characterization of the UV-induced changes in the dye-sensitized solar cell through comparisons of otherwise identical cells in LiI-containing solution and in tetrabutylammonium iodide-containing solution, before and after UV illumination. The "UV effect" is also observed in hydroquinone/benzoquinone solution; thus, it is not dependent on the presence of the I^-/I_2 redox couple. Although surface states are usually deleterious for planar semiconductor electrodes, we show that a high density of surface states may be beneficial for the photoconversion process in nanoporous solar cells.

Introduction

The sensitization of nanoporous, wide-band gap semiconductors by adsorbed dyes[1−3] is becoming competitive with the use of conventional semiconductors for the conversion of sunlight into electrical energy. However, the development of dye-sensitized solar cells, DSSCs, has been so rapid that some fundamental questions remain to be answered even as these cells are beginning to appear in commercial products. Here we address a subject that is increasingly understood to be important to DSSCs and is also relevant to other cells that rely on electron transfer across a semiconductor/solution interface: the effect of surface electronic states on electron transfer and transport processes. Surface states are expected at almost all inorganic semiconductor/electrolyte[4,5] or semiconductor/solid[6] interfaces because the lattice periodicity of the semiconductor is interrupted at the surface leaving "dangling" bonds and/or resulting in rearrangement of the surface atoms. The exceptions are those semiconductors in which the covalent bonds are restricted to two dimensions (e.g., SnS_2); such crystals, when cleaved parallel to the covalent layers, show very low surface state density.[7,8] Surface states are normally considered to be deleterious to the semiconductor's function because they can trap carriers and promote their recombination.

There is clearly a large "intrinsic" surface state density in the nanoporous TiO_2 films used for DSSCs, due simply to the large surface area of the films and to the less than perfect crystallinity of the particles. The intrinsic surface state density has been measured or inferred,[9] and its influence on the photoconversion process has been considered by a number of research groups.[10−15] Although there is not yet a generally accepted understanding of the role of surface states in DSSCs, an emergent theme is that their presence is not always bad. Although subconduction band states usually tend to trap electrons, and thereby influence the transport properties,[2,10−19] their presence may also increase the photoinjection efficiency of the dye and may decrease the interfacial recombination rate.[2,10,17,20−23,24] Because DSSCs are majority carrier devices, trapping of electrons in the TiO_2 does not necessarily increase the recombination rate, as it would for a minority carrier device; it can, in fact, reduce it substantially. In short, the role of surface states in the nanoporous TiO_2 remains a topic of great interest. Here we present the first report of the *reversible* production (and destruction) of photoactive surface states in the nanoporous TiO_2 and detail their effect on the photoconversion properties of DSSCs. These UV-produced states are distinct from the intrinsic surface states. The ability to create at will *observable* surface states, and later to eliminate them, provides an unprecedented opportunity to quantitatively measure the effect of surface states on the dye sensitization process.

In a preliminary communication,[25] we described the "UV effect" in a series of cells that employed different perylene-based dyes[26] and further showed that the effect also appeared in cells sensitized with the more common ruthenium-based dyes. For some of the otherwise poorly performing perylene dyes, brief UV illumination resulted in a *10−45-fold increase* in photoconversion efficiency. This effect led to the highest efficiency yet reported for a perylene-based dye.[25] Interpretation of the UV effect using the perylene dyes was difficult, however,

* To whom correspondence should be addressed.

10.1021/jp022000m CCC: $25.00
Published on Web 02/25/2003

because they tend to aggregate and this can substantially diminish their injection efficiency. It was not known if the UV effect was partially due to disaggregation of the perylene dyes. To more thoroughly characterize this powerful and potentially useful effect, we report here an in-depth study of the UV-induced changes in DSSCs. For clarity, we utilize only bare TiO_2 films or films sensitized with one dye: bis(2,2′-bipyridine)-(4,4′-dicarboxylic acid-2,2′-bipyridine)ruthenium(II), that we refer to as the "tris dye".[25,27] This dye is similar to the most common sensitizing dye for DSSCs, N3(bis(4,4′-dicarboxy-2,2′-bipyridine)ruthenium(II) di-isothiocyanate),[28] but it has a more positive redox potential and a relatively poor photoconversion efficiency in the usual cell. From our earlier work, we knew that DSSCs made with the tris dye underwent substantial improvement in photoconversion efficiency upon UV illumination. Moreover, these changes are unlikely to be caused by disaggregation, as was possibly the case with the perylene dyes.

Some of the key aspects of the UV effect previously reported[25] are summarized here for convienence. (1) Brief UV illumination (1−15 min) of an assembled dye-sensitized solar cell with a non-Li^+-containing electrolyte resulted in long-lasting substantial improvement of the photoconversion efficiency. The effect was minimal or absent in Li^+-containing electrolyte and diminished but still observable in K^+-containing electrolyte. (2) The effect was noticeable, but relatively weak, with dyes that were highly efficient, like N3. However, the effect was dramatic for dyes that otherwise had low efficiencies, like the perylene dyes and the tris dye. (3) The results of the UV effect lasted as long as our unsealed cells retained their electrolyte solution (∼1−2 h). However, the effect disappeared (half-life ∼ 5 min) if the cells were disassembled and exposed to ambient conditions. (4) The effect was completely reversible: a dye-sensitized TiO_2 film's efficiency could be greatly enhanced by exposure to UV in a cell, then returned to baseline efficiency by rinsing and exposure to atmosphere, and then enhanced again by subsequent assembly into a cell and exposure to UV. This cycle could be repeated indefinitely. (5) Air and water were not required for this effect: identical behavior was observed in a helium atmosphere glovebox using rigorously dried solvents and electrolytes.

Experimental Section

Our usual UV illumination of a DSSC involved simply removing the 400 nm long pass filter from the 75 W Xe arc lamp (PTI), whereas the cell was at either short circuit or open circuit (it did not seem to matter). Although both visible and UV illumination were applied, we showed earlier that only the UV changes the cells. Illumination with the 365 nm line of a mercury lamp produced the same effect, and we occasionally employed this source. Unless otherwise mentioned, visible illumination was with the 75 W Xe lamp filtered through 7 in. of water *and* a 400 nm long pass filter. The intensity at the cell surface approximated 1 sun over the range from 400 to 800 nm.

We tested our two normal TiO_2 formulations (synthesized in acetic acid and HNO_3),[27,29] the TiO_2 commercially available from Solaronix, and that from our colleagues (A. J. Frank's group at NREL); all TiO_2 batches showed practically identical UV effects. The dye was synthesized as described previously.[25,27] We employed it in the form that had two protons and two PF_6^- counterions; the dye was adsorbed from dry ∼0.1 mM ethanol solution. Freshly sintered TiO_2 films were immersed while still warm, without rinsing, in the dye solution. Cell assembly and all measurements and characterizations were routine and performed as previously described.[25,27,29,30]

We employ two different electrolyte solutions to characterize the films: (1) 0.5 M LiI, 0.05 M I_2 in distilled 3-methoxypropionitrile, and (2) 0.5 M TBAI, 0.05 M I_2 in distilled 3-methoxypropionitrile (TBAI = tetrabutylammonium iodide). To simplify the presentation, we will often refer to cells with electrolyte (1) as "Li cells" and to cells with electrolyte (2) as "TBA cells". In general, we did not employ 4-*tert*-butylpyridine in the electrolyte solutions[28] in order to minimze the number of variables. However, when we did employ it, we observed no qualitative differences.

Electrochemical potentials are quoted vs the standard calomel electrode, SCE. They were measured using a Ag quasireference electrode that was calibrated for each solution using the ferrocene/ferricenium couple.

Results

TBA^+- and Li^+-Containing Electrolytes. UV illumination of DSSCs can result in a very substantial increase in photoconversion efficiency as long as the electrolyte solution does not contain Li^+ or other ions that specifically adsorb to the TiO_2 surface (potential-determining ions). Ions that weakly adsorb to the TiO_2, such as potassium, allow a weak UV effect to occur.[25] The two electrolyte cations used in this study were chosen because they exhibit almost opposite behavior toward TiO_2 (and other oxide semiconductors). Because of its large size and the nonreactive alkyl groups on its periphery, TBA^+ does not adsorb on the TiO_2 surface nor does it react chemically with it. On the other hand, Li^+ is a potential-determining ion for TiO_2[2,10,24] because it specifically absorbs on the surface, and at negative potentials beyond those used in this study, it intercalates into the TiO_2. The additional positive surface charge from adsorbed Li^+ moves the TiO_2 conduction band edge, E_{cb}, to a more positive potential (thereby enabling more facile electron injection from some adsorbed dyes). Potential-determining ions act for a semiconductor's bandedge potential somewhat like the components of a buffer act for the pH of aqueous solutions: they determine the potential according to their concentration, at least until their "buffering capacity" is overwhelmed. Specific adsorption of Li^+ should cause the conduction band to be more positive than it is in TBA^+ solution.

UV Effect vs Time. The changes caused by UV illumination for up to 15 min are shown in Figure 1 for tris dye-sensitized cells with both TBA^+- and Li^+-containing electrolytes. These results are from a pair of cells, but their behavior is common to all cells we have investigated. The UV-induced changes in the TBA cell are huge (Figure 1a). The short circuit photocurrent density, J_{sc}, increases by a factor of ∼50 after 15 min illumination. As the photocurrent increases, the open circuit photovoltage, V_{oc}, decreases slightly. The dark current onset potential also shifts positive (Figure 1c). In contrast, the effect of UV illumination in Li cells is minimal, even detrimental (Figure 1, parts b and d). The Li cells function very well without UV illumination and are far superior to the TBA cells before UV illumination. Higher V_{oc}'s were obtained in both types of cells when 4-*tert*-butylpyridine was employed.

The changes in photovoltaic parameters in these cells as a function of UV illumination time are shown in Figure 2, parts a−d. The open circuit photovoltage increases at first under UV illumination for the TBA cell (Figure 2a), before eventually decreasing. The fill factor, ff, follows a trend similar to V_{oc}, as expected (Figure 2c). The monotonic increase in J_{sc} coupled to the initial increase and then decrease of V_{oc} and ff leads to a total power, P, that at first increases strongly and then reaches a broad maximum and begins to decrease slowly with continued UV illumination time (Figure 2c).

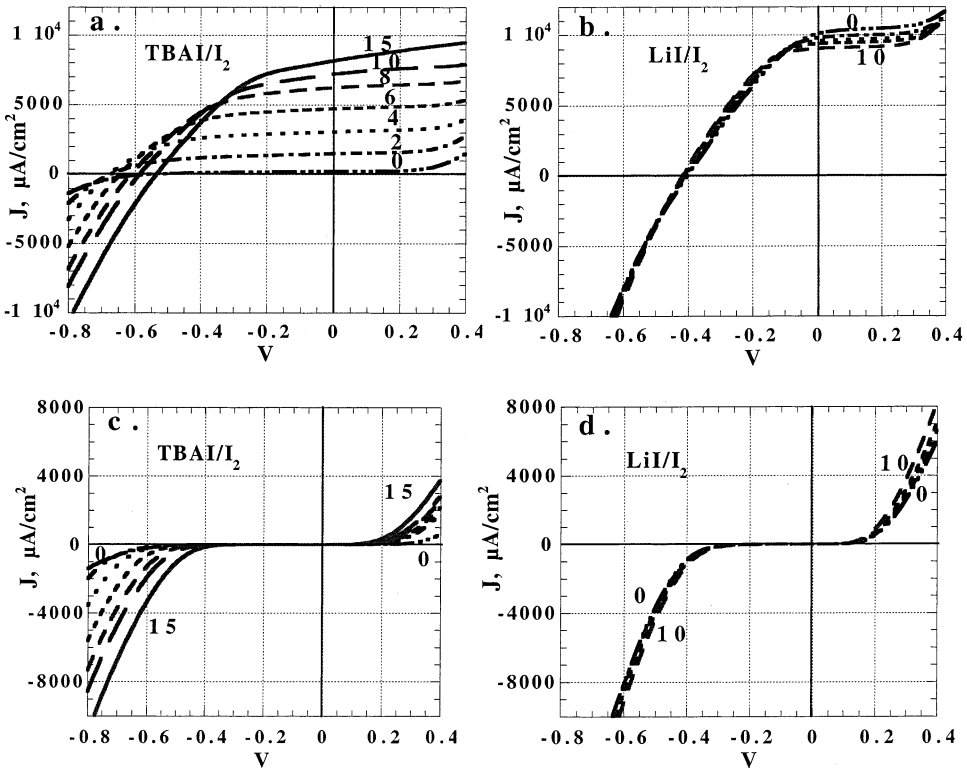

Figure 1. Photocurrent−voltage curves (a and b) and dark current−voltage curves (c and d) for cells in $TBAI/I_2$ (a and c) and LiI/I_2 (b and d) after UV illumination for the indicated times in minutes.

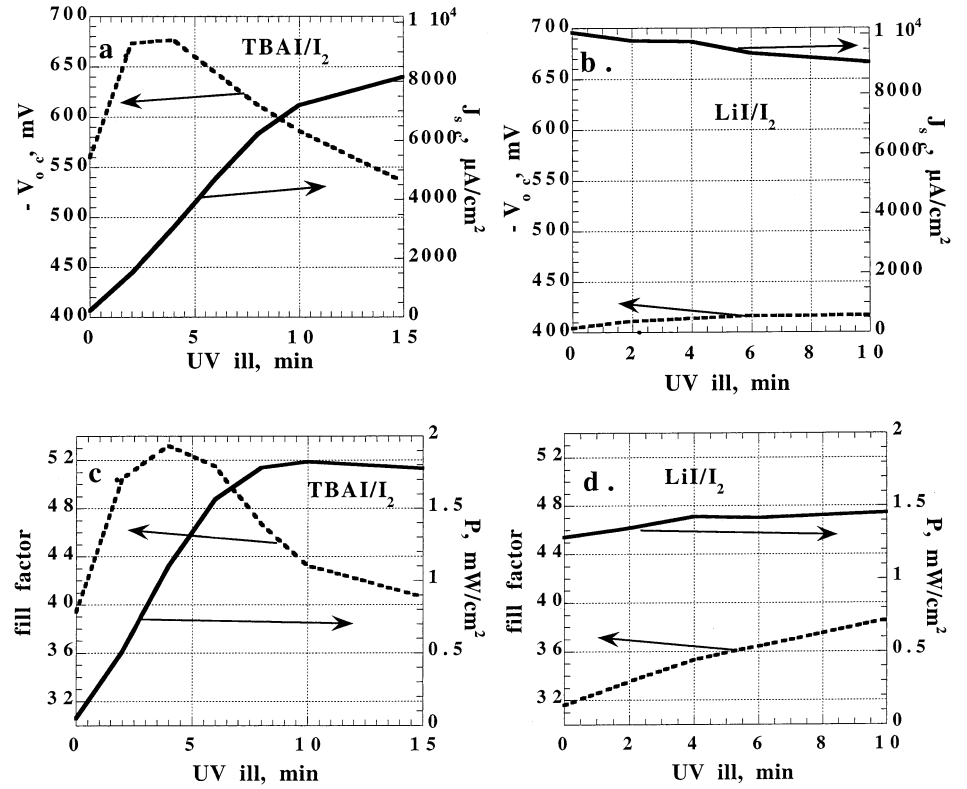

Figure 2. Photovoltaic parameters of the cells shown in Figure 1 as a function of UV illumination time.

Although there is only a small effect of UV illumination on the photocurrents of the LiI/I_2 cell (Figure 2b), it is primarily in the opposite direction as in the $TBAI/I_2$ cells (Figure 2a). The photocurrent of the Li cell decreases slightly, whereas V_{oc} and ff increase slightly following UV illumination. Overall, the power produced by the cell increases slightly upon UV exposure (Figure 2d). Although this cell is far more efficient than the TBA cell before UV illumination, it becomes less efficient after ~6 min UV illumination, primarily because of the higher V_{oc} and ff of the TBA-cell.

UV Effect in an Iodine-Free Redox Couple. Many results show that the LiI/I_2 redox couple has very different properties

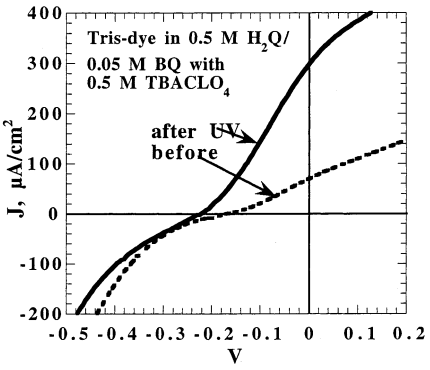

Figure 3. Effect of UV illumination in an electrolyte consisting of hydroquinone (H_2Q), benzoquinone (BQ) and $TBAClO_4$.

than the $TBAI/I_2$ redox couple. It makes intuitive sense that the difference in cations (the potential-determining Li^+ vs the nonadsorbed TBA^+) is responsible for this difference in behavior between these two redox couples.[3,27,29] Usually, DSSCs function efficiently only with the I^-/I_2 couple[31] and somewhat less efficiently with several newly discovered redox couples that also have very slow self-exchange kinetics.[32,33] Nevertheless, we employed a much different redox couple, hydroquinone (H_2Q, 0.5 M)/benzoquinone (BQ, 0.05 M) with 0.5 M $TBAClO_4$, to clarify the role, if any, of I^-/I_2 in the mechanism of the UV effect (Figure 3). This couple is not capable of efficient photoconversion (Figure 3, "before"), but the cell's efficiency is substantially enhanced by exposure to 10 min of UV illumination (Figure 3, "after"). This demonstrates that the UV effect is not dependent on the presence of iodine.

Measuring Bandedge Motion and Its Role in the UV Effect. To measure the changes in $J-V$ behavior that would be caused purely by a positive bandedge shift and to compare them to the UV-induced changes, we employed the pH effect (albeit in nonaqueous 3-methoxypropionitrile solution) to adjust the conduction bandedge position, E_{cb}, of the TiO_2 in a dye-sensitized cell in $TBAI/I_2$ solution. The effective pH was changed by varying the composition (from 100:1 to 1:100) of a pyridine/pyridinium hydrochloride buffer[34] (total buffer concentration 100 mM). This is compared to the changes in $J-V$ behavior caused by UV illumination in the same $TBAI/I_2$ electrolyte solution without buffer (Figures 4a and b).

UV Effect in Bare TiO_2 Films. Spectroelectrochemical measurements in nanoporous TiO_2 cells without a sensitizing dye were previously employed to estimate E_{cb} in nanocrystalline TiO_2.[22,44] We also employed this technique in 0.1 M $LiClO_4$-containing cells and 0.1 M $TBAClO_4$-containing cells before and after exposure to 15 min UV illumination (Figure 5). The cells were ~2 mm thick and contained ~1.0 mL of electrolyte solution.

The absorption spectra of the two cell types under strong negative bias (−1400 mV vs SCE) are shown in Figure 5b. The Li cell shows the spectrum expected from previous studies[22,44] with an absorption peak near 700 nm. The TBA cell shows a stronger absorption at both shorter and longer wavelengths and a broad peak near 850 nm.

The bare anatase TiO_2 nanostructured electrode has a band gap of ~3.2 eV and thus should absorb only photons of $\lambda <$ 390 nm. We measured dark currents of the bare electrodes as well as the photocurrents produced by sub-bandgap illumination of $\lambda >$ 400 nm before and after 15 min UV illumination in both TBA^+- and Li^+-containing solutions (Figure 6). Before UV illumination, the photocurrents ($\lambda >$ 400 nm) were practically zero in both cells (Figure 6, parts a and b). However,

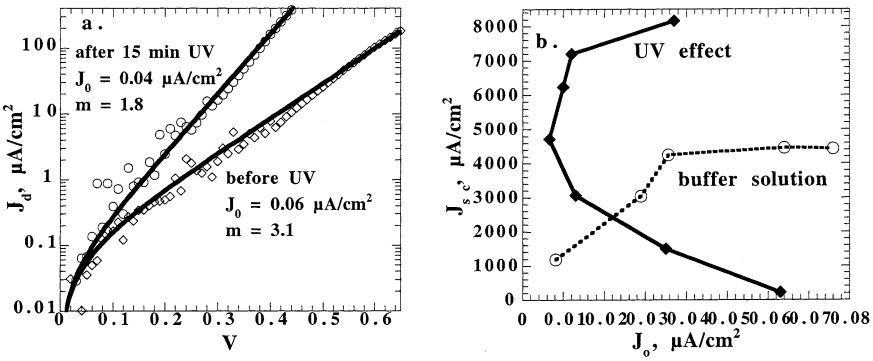

Figure 4. (a) Dark currents, J_d, in unbuffered dye-sensitized TBA cells before and after UV illumination. Data are fit to the diode equation (eq 1) and the resulting parameter values are shown. (b) The change in the short circuit photocurrent density, J_{sc}, induced by (circles) adjusting the ratio of pyridine to pyridinium hydrochloride buffer or by (diamonds) UV illumination for various times (0−15 min) without buffer. The results are plotted versus the exchange current density, J_o, obtained by fitting the dark currents to the diode equation.

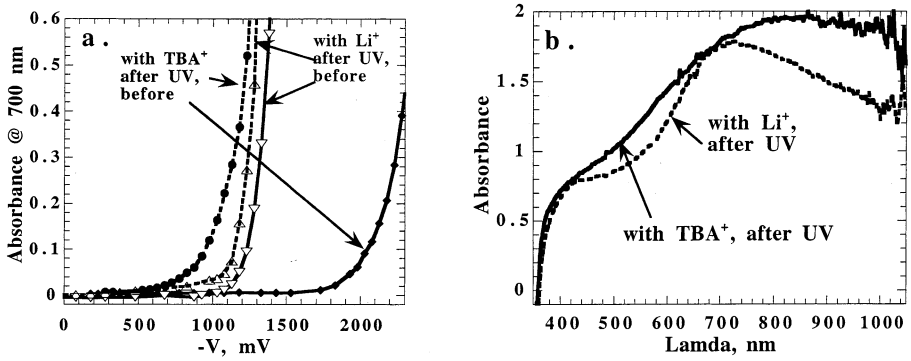

Figure 5. (a) Absorbance of bare TiO_2 films at 700 nm, before and after UV illumination, as a function of applied potential vs SCE. (b) The absorption spectra after UV illumination of the TBA cell and of the Li cell at −1400 mV.

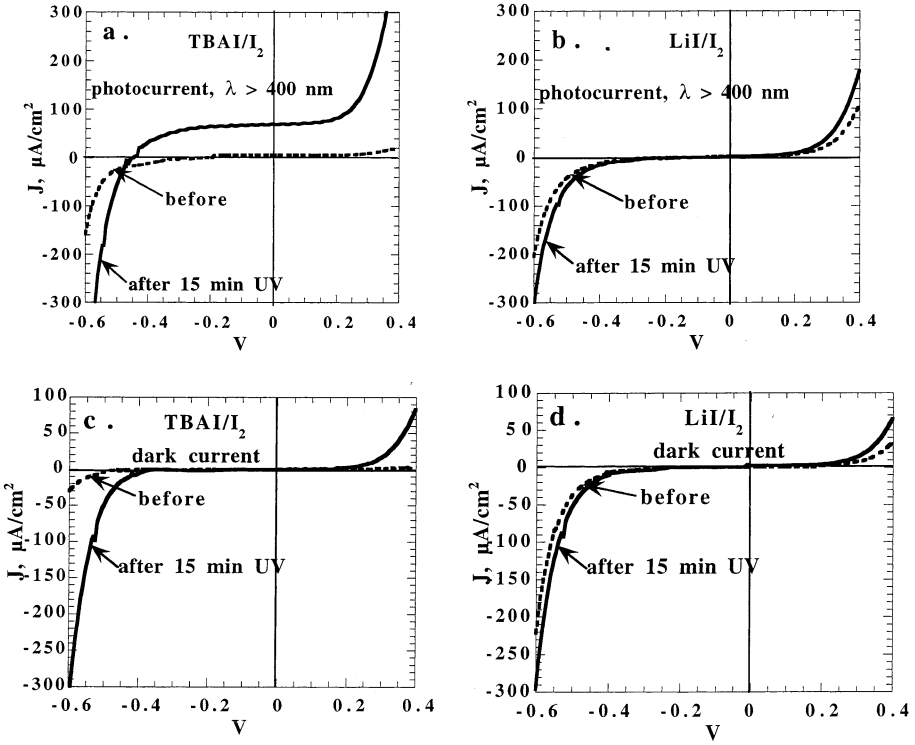

Figure 6. Photocurrents (λ > 400 nm) (a and b) and dark currents (c and d) of bare, nanostructured TiO_2 cells before and after 15 min of UV illumination.

after UV illumination, a remarkable increase in photocurrent was observed in the TBA cell (Figure 6a), whereas still practically no photocurrent was measured in the Li cell (Figure 6b). The change in the photocurrents was also reflected by changes in the dark currents: there was a marked increase in J_d in the TBA-cell (Figure 6c) but little change in the Li cell (Figure 6d).

UV-Induced Production of Photoactive Surface States. The surprising increase in photocurrent under visible light irradiation (λ > 400 nm) after UV illumination of the TBA cell (Figure 6a) shows that photoactive sub-bandgap states are created upon UV illumination. Photocurrent action spectra (that is, incident photon to current efficiency, IPCE, spectra) also clearly revealed these states and revealed a fundamental difference between the TBA cells and the Li cells (Figure 7).

In both TBA and Li cells, IPCE measurements before UV illumination showed the expected spectrum of a semiconductor with a ~3.2 eV band gap. Both spectra are identical before UV illumination, showing that neither Li^+ nor TBA^+ by itself perturbs the photoactive electronic structure of the TiO_2 surface. However, after UV illumination, the bare TiO_2 films produce a ~10−100 fold increase in photocurrent below E_{cb} in the TBA-cells (Figure 7a), whereas a slight *decrease* in photocurrent is observed in the Li cells (Figure 7b).

To further establish a connection between the UV effect in dye-sensitized cells and the UV-induced surface state density in the bare TiO_2 cells, we measured the decay times of the short circuit photocurrent (λ > 400 nm) *in sealed cells*, both bare TiO_2 and dye-sensitized, as a function of time after a 15 min illumination with UV. We reasoned that if the UV effect in the dye-sensitized cells was correlated with the UV-induced surface states seen in the bare TiO_2 cells they should have similar decay times. These experiments also serve the independent goal of measuring the longevity of the UV-induced changes in the cells. Figure 8 shows that decay times for both dye-sensitized cells

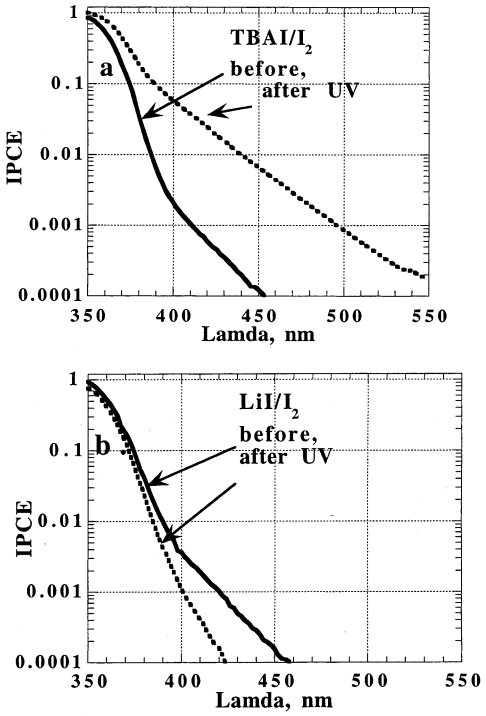

Figure 7. Photocurrent action (IPCE) spectra of bare TiO_2 films before and after UV illumination for 15 min. Photoactive surface states are reversibly created by UV illumination in TBA cells (a), whereas they are diminished in Li cells (b). If the cells are disassembled, rinsed, and reassembled, they return to the "before" curves.

and bare TiO_2 cells after UV illumination are very similar. The UV effect decays by ~25% in the first ~5 h and then much more slowly. After 2 months, it decreased by ~80%.

The IPCE spectra of the tris dye-sensitized TBA cells, before and after UV illumination, are shown in Figure 9. The photocurrent quantum yield increases substantially upon UV

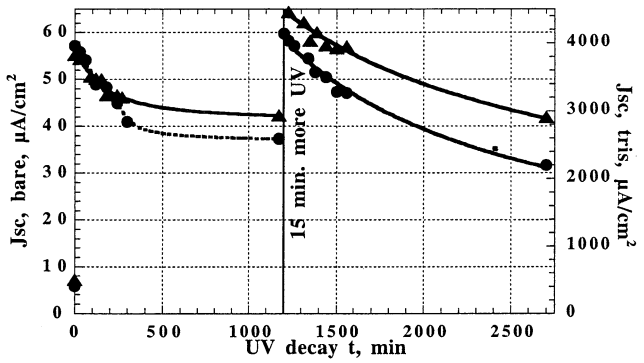

Figure 8. Decay of the UV effect, as expressed by the short circuit photocurrent density as a function of time for both the bare TiO_2 cell (triangles, left axis) and the dye-sensitized cell (circles, right axis) in sealed cells with $\lambda > 400$ nm. Data points are an average of two cells apiece. At 1200 min (20 h), the cells were exposed to another 15 min of UV illumination. The original values before UV illumination are shown on the left ordinate at zero minutes.

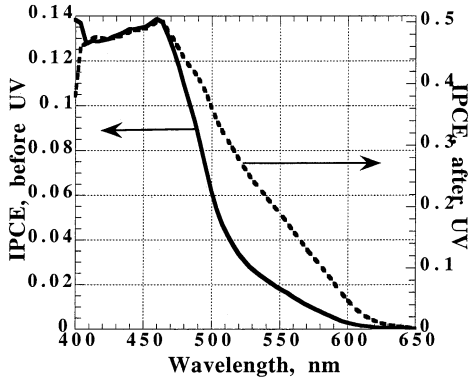

Figure 9. IPCE spectra of a tris-dye-sensitized TBA cell before and after UV illumination for 10 min.

illumination and the long wavelength response increases much more than the response at the peak absorption wavelengths.

Discussion

Bandedge Motion. The results shown in Figures 1a,c and 2a,c for the TBA cells seem to suggest that UV illumination leads to a positive shift of the TiO_2 bands, thereby enhancing dye photoinjection and decreasing V_{oc}. However, this is only part of the story: the actual effect is more subtle and complex. UV illumination of the Li cells (Figures 1b,d and 2b,d) has only a small effect: many of our results show that the presence of Li cation inhibits the UV effect. As mentioned in our previous publication,[25] other specifically adsorbing, and therefore, potential-determining, ions such as Na^+ and K^+, also inhibit the UV effect, but Li^+ inhibits it the most and K^+ the least. A modest UV effect, less than half the level observed in TBA solution, is observed in K^+-based electrolyte.

In our original communication[25] we suggested that UV-induced positive bandedge motion of the TiO_2 played an important role in the UV effect, but we also knew that there had to be at least one other factor to explain the results. Here we show that bandedge motion probably plays a role but that it is difficult to quantify its effect in a functioning cell. Furthermore, the other factor (the production of surface states) has now been identified and clearly linked to the UV effect. The bandedge position of oxide semiconductors such as TiO_2 are sensitive to pH,[4,5] usually moving negative by approximately 59 meV per pH unit (in aqueous solution at room temperature) because of the increasingly negative surface charge caused by removing or neutralizing H^+ groups and adding OH^- groups.

Unfortunately, there are no direct measures of the equilibrium bandedge position in a functioning DSSC, and therefore, we can employ only indirect methods for estimating it (Figure 4). Because of its importance, we discuss this problem in some detail. We used to believe,[25] with others,[35] that the relative bandedge positions in DSSCs could be estimated by comparing the V_{oc}'s under conditions where the J_{sc}'s were set equal (by adjusting light intensities). This was the rationale for our earlier conclusion that bandedge motion played a major role in the UV effect. However, we now understand that the bandedge position in a functioning device cannot be so easily estimated. The foregoing procedure implicitly assumes that the diode quality factor, m, for the devices under comparison are identical, and this is usually not true. The dark current density, J_d, of a diode is given by the diode equation

$$J_d = J_o \exp(qV/mkT - 1) \qquad (1)$$

where J_o is the exchange (or reverse saturation) current density, q is the electronic charge, V is the applied voltage, and kT is Boltzmann's constant times the absolute temperature. Equation 1 shows the strong effect of m on the J_d-V curve and, by extension, on the photo $J-V$ curves.

Using numerical simulations (SimWindows[36,37]) of a silicon p−n junction solar cell (the best-understood solar cell), we showed that changing *just* the carrier mobility results in changes of both m and V_{oc} (data not shown). Plotted at constant J_{sc}, V_{oc} can change substantially with no change in bandbending. This proves that it is not possible in general to measure changes in bandedge position, or bandbending, solely by measuring changes in V_{oc} at constant J_{sc}. This procedure is valid *only* if m remains constant (which is not the case in the UV effect). Changes in effective carrier mobilities, recombination rates, or bandedge motion resulting from illumination or applied voltage will cause changes in m. We now employ an improved, but still approximate, method for estimating changes in E_{cb}.

The diode equation may seem to be inappropriate to DSSCs because there is no band bending and no space charge layer in a DSSC, however, the equation is valid for semiconductor electrodes even in the *absence* of an electrical junction. Equation 1 simply describes the exponential increase in current with driving force, qV, that is characteristic of interfacial electron-transfer reactions.[38] Because it is based on electron transfer theory[39] and does *not* require the existence of an electrical junction, it applies at least semiquantitatively to all semiconductor electrode systems. It is also formally equivalent to the Butler−Volmer equation that is used for electrochemical systems.[38] Conversely, the fact that the current−voltage characteristics of a device can be fit to the diode equation does not mean that it contains an electrical junction.[40−42] We employ the diode equation as a tool to semiquantitatively describe the dark current characteristics of DSSCs as they are altered by UV illumination. The major factor that limits the quantitative applicability of eq 1 to DSSCs is the nanoporous nature of the TiO_2 film that results in a distribution of potentials, V, across the film.[3,27,43]

The measured current density for electrons, $J_e = n_e\mu_e\nabla E_{fn}$, is given by the free electron density, n_e, times the electron mobility, μ_e, times the gradient of the electron quasi Fermi level, ∇E_{fn}. Similarly, the exchange current density, J_o, (eq 1), which is the magnitude of the equal and opposite current fluxes across the interface at equilibrium, is proportional to n_e. The absence of bandbending in DSSCs simply means that the electron density at the surface is the same as it is in the "bulk". The electron

density at equilibrium is given by

$$n_e = N_c \exp[(E_{cb} - E_f)/kT] \quad (2)$$

where N_c is the density of states at the bottom of the semiconductor conduction band. Through n_e, therefore, J_o is a measure of the energy difference between the equilibrium Fermi level, E_f, and the conduction bandedge, E_{cb}. This provides a method for estimating changes in E_{cb}. It is (also) not exact because changes in the interfacial electron-transfer rate constant, k_{et}, can result in changes in J_o. However, because the redox couple, I^-/I_2, remains the same in all of our experiments, k_{et} is unlikely to change substantially, whereas we now know that m (used in the previous method) does change substantially.

The redox couple, I^-/I_2, fixes the potential of E_f in the TiO_2 film. Thus, measuring the change in J_o (by fitting dark currents to eq 1) as a function of UV illumination time is a measure of the change in E_{cb} (at constant k_{et}): increasing J_o indicates a positive shift of E_{cb}, and vice versa. Representative fits to eq 1 of dark currents before and after 15 min of UV illumination in TBA cells are shown in Figure 4a. The dark currents were fitted to eq 1 only up to $J_d \approx 0.4$ mA/cm^2 to minimize any effects from mass transfer resistances. The results show that the slopes (proportional to m) of the curves change substantially under UV illumination, whereas the current "onsets" (proportional to J_o) are almost identical. Specifically, m decreases monotonically from $m = 3.1$ at $t = 0$ min to $m = 1.8$ at $t = 15$ min UV illumination of the cell shown in Figure 4a, whereas J_o changes only slightly, $0.06 \rightarrow 0.04$ μA/cm^2. This qualitative behavior was observed in all cells, although many had a somewhat smaller change in m than the cell shown in Figure 4a. Significantly, in all cells, J_o at first decreased (indicative of *negative* bandedge motion) and then increased again (positive bandedge motion) during UV illumination (Figure 4b). Overall, the total change in E_{cb} appeared to be small (assuming constant k_{et}).

The dark currents of cells with different buffer concentrations were also fit to eq 1 (not shown) and revealed a much different behavior than the cells exposed to UV. They show a set of almost parallel curves (constant m) displaced along the current axis (increasing J_o, Figure 4b). In contrast to the UV-illuminated cells, m changes only slightly, $2.2 \rightarrow 2.0$, over the range in buffer concentration. However, J_o changes monotonically by an order of magnitude, $0.008 \rightarrow 0.08$ μA/cm^2. This is consistent with a positive bandedge shift caused by increasing buffer acidity and no change in interfacial or bulk electronic properties. In short, the behavior of the buffered cells is very different than that of the UV-illuminated cells.

Because of the uncertainties involved in this analysis, we do not attempt to quantitatively interpret the results shown in Figure 4. However, the fitting procedure seems reasonable, giving the results expected for the buffered cells. Furthermore, it suggests that the UV effect is probably only weakly correlated to positive motion of E_{cb}.

In Li cells, with or without UV, m is near 1.7 and J_o is near 0.14 μA/cm^2, consistent with a bandedge position more positive than ever achieved in TBA cells. Fortuitously, the value of m after 15 min UV illumination in TBA cells (Figures 1c and 4a) is about equal to that of the corresponding value in Li cells (Figure 1d), and the two J_{sc}'s are also about equal. Therefore, it is valid, *in this case*, to relate V_{oc} to the relative bandedge positions. This leads to the conclusion that E_{cb} *in the TBA cell after UV illumination is at least* ~120 meV negative of E_{cb} in the Li cell. This accounts for the higher photovoltage achieved in TBA cells.

Knowing what factors cause a decrease in m suggests that one or more of the following plays a major role in the UV effect: (1) electron transport through the TiO_2 becomes more facile (this is supported by the increase in the long-wavelength IPCE shown in Figure 9), (2) interfacial charge transfer, k_{et}, to I_2 and/or I_3^- becomes more rapid (although this by itself would *decrease* J_{sc} and V_{oc}), and/or (3) the magnitude of the bandedge motion resulting from an applied or photogenerated carrier concentration is reduced. It is worth noting for factor 3 that the interfacial capacitance of TBA cells is much lower than Li cells because of the much larger size of the TBA^+ ions. Therefore, substantial bandedge motion is far more likely to occur in TBA cells.[3,27] Upon illumination of TBA cells (before the UV effect), the negative bandedge motion caused by the accumulation (trapping) of photoinjected electrons might tend to turn off further injection, leading to low photocurrents but high photovoltages (Figure 1a, 0 min). One partial explanation for the UV effect in TBA cells is that it may greatly increase the mobility of photoinjected electrons (see below) and thereby mostly prevent photoinduced negative bandedge motion of the TiO_2[3,43] while promoting more efficient photoinjection from the dye. We now discuss the change in photovoltaic properties of the bare TiO_2 films.

UV Effect in Bare TiO_2 Films. The onset of electro-induced absorption (Figure 5a) is strongly shifted to more positive potentials (by ~1 V) after UV exposure of the TBA cell, whereas the Li cell is only weakly affected. This may seem at first to indicate a strong positive shift of E_{cb} upon UV illumination of TBA cells, but this explanation is too facile. For one thing, it contradicts our earlier conclusion that E_{cb} in UV illuminated TBA cells must be at least ~120 meV *negative* of E_{cb} in Li cells. The problem is that the spectroelectrochemical measurement (Figure 5a) provides the potential at which a measurable quantity of "free"[22,44] electrons appear in the TiO_2, but this is not a measure of E_{cb} *at equilibrium*, which is the quantity of interest. It is hardly likely that the equlibrium E_{cb} in TBA cells before UV illumination is ~ −1.8 V vs SCE, as it would seem to be from Figure 5a. If it were, no normal dye could inject into it. However, even the relatively positive tris dye injects into it (Figure 1a), as do substituted phthalocyanines with no acidic binding groups (not shown). The simplest explanation is that E_{cb} is not pinned in TBA solution; therefore, application of a negative potential to the TiO_2, or injection of electrons from dyes, causes negative bandedge motion,[27,29,43] and if a dye is bound to the surface, its potential will follow, to some degree, the change in the TiO_2 potential.[27,43] On the other hand, because Li^+ is a potential-determining ion, it tends to pin E_{cb} at a positive potential, and it will intercalate, and thus chemically change the TiO_2, if the potential moves too far negative. The most likely explanation for the results of Figure 5a, and one strongly supported by our other results, is that the negative bandedge motion of the TiO_2 in the TBA cells is strongly inhibited by UV illumination (via the generation of surface states, see below). Therefore, the data of Figure 5a, although qualitatively useful, do not provide a measure of the *equilibrium* E_{cb}. In fact, E_{cb} of the TBA cell after UV illumination is almost certainly substantially negative of E_{cb} in the Li cell. The early onset of absorbance in the TBA cell is evidence of surface state filling, not of the equilibrium position of E_{cb}, and the spectrum of these filled states is different from the spectrum of what are presumably filled conduction band states in the Li cell (Figure 5b).

UV-Induced Production of Photoactive Surface States. The surprising increase in photocurrent under visible light irradiation

($\lambda > 400$ nm) after UV illumination of the TBA cell (Figure 6a) shows that photoactive sub-bandgap states are created upon UV illumination. We attempted to observe the empty states directly by absorption spectroscopy but could not, probably because of the strong light scattering of the nanoporous films. However, the absorption of the filled states could be observed (Figure 5b).

The change in TBA-cells upon UV illumination (Figure 7a) is a highly unusual result that reveals visually the presence of photoactive *surface* states (we justify this assignment below). Most commonly, the presence of semiconductor surface states is not directly seen and only can be inferred via indirect measurements and comparison to theory. However, here we observe a clear spectroscopic signature of a large density of photoactive surface states that can be produced by UV illumination and eliminated again by exposure to ambient air. The UV-produced photocurrent, increasing by 10−100 fold at energies up to 1 eV below E_{cb} (=388 nm), is nearly as high as the photocurrent produced by irradiation *above* the band gap energy, showing that the UV-induced surface state density is extremely large. This high density of sub-bandgap states suggests comparisons to the electronic structure of amorphous silicon. In a-Si,[45] one speaks of a mobility edge rather than a bandedge, because there are electronic states distributed throughout what would otherwise be called the band gap. (A similar description may be appropriate to conducting polymer-based solar cells.[46−48]) Once the density of intragap (or surface) states becomes large enough to accommodate carrier transport, conduction can occur primarily through these sub-bandgap states: therefore, the notion of a distinct bandedge is no longer truly relevant. In the UV-illuminated nanoporous TiO_2 films, *the mobility edge may be described as the percolation threshold of surface states*, that is, as that energy level at which the surface state density becomes high enough to support a current flux. This high density of surface states also makes the film more n-type and therefore more conductive. This results from the decreased energy difference between the Fermi level and the lowest available electronic state (eq 2).

The connection between the UV-induced surface states in bare TiO_2 (Figure 7a) and the UV effect in dye-sensitized films (which cannot be proven directly) is strongly supported by the fact that the distinguishing five aspects of the UV effect described in the Introduction are exactly correlated with the presence or absence of the UV-induced surface states (some of these data are presented here, some were presented earlier[25]). The rise of the surface state-produced photocurrent has the same time dependence in bare TiO_2 as does the increase in the DSSC. They also share the same decay kinetics upon opening and rinsing the cells. Unfortunately, we cannot directly observe the TiO_2 surface states in a dye-sensitized cell because of the strong dye absorption in the relevant spectral region. Therefore, the experiments shown in Figure 8 were performed showing that the decay in sealed cells of the UV-induced surface state density in bare TiO_2 films was practically identical to the decay of the UV effect in DSSCs. These data, along with the data presented earlier, strongly suggest that the UV effect in dye-sensitized cells is directly correlated to the UV-induced surface state density in bare TiO_2 cells.

Surface States in Planar, and in Nanostructured, Semiconductors. In planar (conventional) semiconductor electrodes, surface states are almost always harmful. Because there is no direct physical connection between the surface and the substrate electrical contact, surface states are always trap states, regardless of their concentration. Ionization of the surface states (say, their filling by electrons) results in charging of the surface and bandedge motion (Fermi level pinning). In general, one concludes that a higher density of surface states leads to a greater degree of bandedge motion under illumination. However, this conclusion is not fundamental; it applies only to *planar* semiconductor electrodes. Bandedge motion is caused by the steady state *charge* density at the surface and not by the surface state density alone.

In nanostructured semiconductor electrodes, the surface extends throughout the "bulk". Therefore, surface states can be in direct electrical contact with the substrate. Before UV illumination, most surface states in the nanoporous TiO_2 may be isolated traps which, when charged with electrons, move the bandedge negative. However, further increasing the density of surface states in DSSCs may lead to electrical communication between the surface states and thereby ultimately to an *improved* conducting pathway to the substrate—a "mobility edge" as described above. Therefore, increasing the surface state density by UV illumination can, in principle, lead to *less* bandedge motion in DSSCs because it results in improved carrier transport and *decreased charge density* at the surface.

The apparent negative shift in E_{cb} upon first illuminating a DSSC with UV, followed by the positive shift with longer illumination time (Figure 4b), may be explained similarly. Because the low density of surface states generated at first will be isolated traps, they should move the effective bandedge negative when charged with electrons. However, as more surface states are created and they begin to coalesce into a mobility edge, the effective bandedge moves positive from E_{cb} to the mobility edge, and carrier transport may become more efficient, thus decreasing the total charge on the surface. This mechanism is obviously still speculative, but it is consistent with all of our results.

Physical Characterization of the UV-Induced Photoactive Surface States. There are a number of considerations that lead us to assign the UV-induced electronic states to surface states rather than to bulk intragap states. (1) The TiO_2 particles are highly crystalline, suggesting that the defect density in the bulk should be low. (2) The particles are so small (~15 nm diameter) that they have a very high surface-to-volume ratio, and defects are much more common on the surface than in the bulk of crystalline materials. (3) The dramatic difference between TBA^+ (a nonadsorbing ion) and Li^+ (an adsorbing ion) suggests that the effect is governed by the TiO_2 surface. (4) The rapid disappearance of the effect upon exposure to ambient atmosphere, far faster than expected from a bulk diffusion process, again suggests a surface effect. Thus, we conclude that the UV-induced sub-bandgap states are surface states.

It is important to determine if these surface states lie below the conduction band or above the valence band. Once created by UV, they are optically observable and have a strong absorption coefficient (Figures 6 and 7); therefore, they must derive from either a filled (valence) band → empty surface state transition or from a filled surface state → empty (conduction) band transition. Although the data of Figures 6 and 7 cannot distinguish between these two possibilities, the IPCE spectra of a dye-sensitized cell before and after UV illumination can (Figure 9). The large increase in photocurrent at wavelengths where the UV-illuminated TiO_2 by itself is not efficient ($\lambda > 450$ nm) shows that J_{sc} is greatly increased after the UV illumination. This strongly suggests that the UV-induced surface states in the TiO_2 must reside in the energetic region accessible to the dye, that is, between the conduction bandedge and the dye's oxidation potential. Otherwise, it is hard to envision how

surface states created outside this region (i.e., near the valence band of the TiO_2) could so dramatically affect the dye sensitization process. Therefore, we conclude that the UV-induced surface states extend below the conduction band edge of the TiO_2 and that their absorbance is due to a valence band → empty surface state optical transition.

Figure 7a shows a smooth progression of photocurrent vs wavelength extending ~1 eV below the conduction band edge. This shows that a corresponding distribution of UV-created surface states exists over this range of energy. The optical transition corresponds to the promotion of an electron from the valence band into the empty (i.e., above the Fermi level) surface state; from this state, the electron must be thermally promoted above the mobility edge to contribute to the measured photocurrent. The photocurrent data of Figure 7a, therefore, are not a direct measure of the distribution of surface states but are convoluted by the fraction of filled states under illumination that thermally populate a state above the mobility edge.

Chemical Characterization of the Surface States. The chemical nature of the intragap state most commonly observed in TiO_2 films has been identified as a Ti^{3+} state.[10] It is believed to increase the rate of recombination of electrons in the TiO_2 with the oxidized iodide species, I_2 and/or I_3^-.[10,11,49] However, it is highly unlikely that the surface states produced by the UV effect are Ti^{3+} states. Because normal dye sensitization by visible light injects a high density of electrons through the TiO_2 and no changes occur, the UV-induced changes must be driven by the presence of UV-created holes in the TiO_2.[25] It is doubtful that a reduced state like Ti^{3+} can be formed as a result of a hole-driven process. In fact, the hole-driven UV effect may tend to oxidize existing Ti^{3+} states back to Ti^{4+}, thereby changing one type of surface state into another. Another possibility we considered are the oxygen vacancies known to be produced by UV illumination of TiO_2.[50] These lead to the amphiphilic surfaces that may be useful for self-cleaning windows, etc. However, these states decay on the order of weeks under ambient conditions, whereas our UV-induced states decay within ~5 min under the same conditions. So it is doubtful that the UV-induced surface states reported here are chemically equivalent to either the Ti^{3+} states or the oxygen vacancies previously reported.

There have been other reports of UV-induced changes in the TiO_2 films used in DSSCs. O'Regan and Schwartz reported a UV-driven enhancement in a DSSC analogue made with the solid-state hole conductor CuSCN.[35] However, their UV effect had much different characteristics than ours, and they attributed it to oxidation and decomposition of the CuSCN hole conductor. Hagfeldt et al. reported the positive bandedge motion of nanoporous TiO_2 films under UV illumination.[51] These bandedge shifts, however, appeared to occur only under *continuous* UV illumination, whereas what we are reporting here is a semipermanent change in the structure of the TiO_2 caused by very brief UV illumination. Hagfeldt et al. reasonably attributed their results to trapped holes at the TiO_2 surface which shifted the bandedge positive. In our case, however, the UV effect is stable for weeks in the presence of 0.5 M I^-, an efficient hole scavenger. Thus, we conclude that the effect cannot be caused by trapped holes. In short, we have found no literature precedent for the surface states we are describing.

The electrical charge on the UV-produced surface states is another important parameter. By simple considerations, we conclude that the empty surface states are primarily electrically neutral: the majority of the surface states are above the Fermi energy (near the conduction band); thus, they are empty of electrons at equilibrium. If the empty states were positively charged, the presence of such a large (Figure 7a) density of positive charges would shift the conduction band strongly positive. However, this is not compatible with the increased (negative) V_{oc} in TBA cells compared to Li cells (Figures 2 and 6). Similarly, if the empty states were negatively charged, this would cause the conduction band to move strongly negative. This, however, would eliminate photoinjection from dyes that have relatively positive excited state injection potentials, like the tris dye. Therefore, we conclude that the UV-produced surface states are primarily electrically neutral because no major shift in the conduction bandedge potential is observed upon their creation.

Mechanism of the UV Effect. We cannot yet provide a proven mechanism, but we can provide a reasonable, self-consistent mechanism that explains the results. The principal result that we must explain is the large (up to 50-fold) increase in short circuit current density, J_{sc}, caused by UV illumination of TBA cells. In principle, this can be caused by one or more of three factors: increased photoinjection efficiency of the dye, decreased carrier recombination, and/or improved carrier transport through the TiO_2. The production of a high density of surface states in the nanoporous TiO_2 film seems to be the primary effect of UV illumination and is most likely the major cause of the resulting increase in photoconversion efficiency. Inducing a large density of surface states below the conduction bandedge can result in carrier motion through the sub-bandgap surface states if the density of induced surface states is high enough to support carrier transport. The resulting mobility edge, to borrow a concept from amorphous silicon research, is equal to the percolation threshold of surface states. The production of surface states mimics a positive shift of the conduction bandedge (Figures 1a,c, 2a,c, 5a, and 6a,c) and/or a decrease in the effective band gap of the semiconductor (Figures 6a,c and 7a). It may also provide new, lower-energy conduction pathways for carriers that would otherwise be confined to trap states, thereby increasing the average carrier mobility and *decreasing* the charge density in the film. For example, UV illumination of an *N3*-sensitized TBA cell (data not shown) did not change the already high (~75%) IPCE spectra, but *did* substantially increase J_{sc} at 1 sun. The increase in the long wavelength IPCE shown in Figure 9 is also compatible with an improved conductivity caused by UV illumination. These and other results suggests that UV illumination leads to improved carrier transport at high light intensities. Somewhat counterintuitively, the UV effect thus may improve the transport properties by *increasing* the "defect" density (this is possible only in nanoporous electrodes, as discussed earlier). More rapid transport, of course, should also result in diminished carrier recombination.

Electron injection from the sensitizing dye is also expected to be enhanced by the UV-induced increased density of available empty electronic states, many of which reside in the formerly forbidden gap. Injection into the higher energy states that are above the mobility edge can lead directly to photocurrent production. It is not known how rapidly carriers relax through the surface states, but some carriers will eventually fill the states below the mobility edge, and some injection may also occur directly into these localized states. These carriers may not contribute substantially to the photocurrent. The "intrinsic" surface states are known to mediate the recombination reaction,[11] but it is not yet clear how the rate of the recombination process is affected by the UV-induced surface states. It is possible that some, or all, of the intrinisic surface states are eliminated by UV illumination and transformed into the photoactive states seen

in Figure 7a. Overall, it seems plausible that the UV-induced surface states play a beneficial role in at least two respects: they may increase the injection efficiency of many dyes, and they may improve carrier transport. It is almost certain that they also play a role in the recombination process, but we do not yet know if it is beneficial or detrimental.

The importance of the effective bandedge position on the photoconversion process is obvious, as is the difficulty in measuring it exactly. The bandedge position is controlled by the quantity and type of ions present in the cell, by the surface state density and by the illumination intensity.[3,27,43] The ability to adjust both the effective conduction bandedge position and its degree of motion by the UV effect allows a far greater degree of control over the photovoltaic properties of DSSCs than has been possible previously. As one interesting example, it is often lamented that the I^-/I_2 redox couple (the only truly viable couple so far) has a potential too far negative to make an efficient DSSC, but this assumes incorrectly that E_{cb} is a fixed quantity. From our studies, we conclude that it is probably easier to maximize the efficiency by adjusting E_{cb} than it is by changing the redox couple.

Summary and Conclusions

DSSCs containing TBAI/I_2 electrolyte solutions are often not very efficient. However, UV illumination of these cells for 10−15 min can improve their efficiency by more than an order of magnitude. This improvement is long-lived and might be made permanent if the mechanism were better understood. The major change in the cells appears in the nanoporous TiO_2 rather than in the dye or the electrolyte. UV illumination leads to the reversible production of a very high density of TiO_2 surface states that is optically observable. This unprecedented result affords the first opportunity to clearly measure the effect of surface states on the interfacial electron-transfer process. So far, these studies have led to the counterintuitive conclusion that these surface states *promote* the photoconversion process. Higher efficiencies can be obtained in UV-illuminated TBA cells than in otherwise identical Li cells (which are almost unaffected by UV illumination).

A practical advantage obtained from the UV effect is the ability to adjust the essential photoconversion parameters, J_{sc}, V_{oc}, ff, etc., to maximize the conversion efficiencies. The more important benefit may be to use this ability to understand the factors that control J_{sc}, V_{oc}, and ff in DSSCs. We discussed in detail the methods used for estimating the equilibrium semiconductor bandedge potential, E_{cb}, and suggest that there is no existing method that is generally capable of determining it in functioning cells. However, if the diode quality factor, m, and the short circuit photocurrent density, J_{sc}, are the same for two cells, then the difference in measured photovoltages, V_{oc}, should correspond to the difference in bandedge potential, E_{cb}. Using this method we conclude that E_{cb} in TBA cells after UV illumination is at least ~120 meV negative of E_{cb} in Li cells. This difference provides the higher V_{oc} in TBA cells, and it also demonstrates the failure of some existing methods to accurately estimate E_{cb}. Using a reasonable, but still approximate, method to compare the change in E_{cb} resulting from use of a nonaqueous buffer solution to the change caused by the UV effect, we conclude that the change in E_{cb} is a small part of the UV effect; the major part of it is related to the UV-induced generation of a large density of surface states.

The UV induced surface state density in TBA cells is so high that it seems to form a percolation threshold for conduction below the formal conduction bandedge. This percolation threshold is similar to the mobility edge found in amorphous silicon devices and can mimic a positive bandedge shift. The large (10−50-fold) increase in J_{sc} resulting from UV illumination can be caused by one or more of three factors: (1) The injection efficiency of the sensitizing dye increases, probably because of the increase in the density of available electronic states; (2) the recombination rate of injected carriers decreases; and/or (3) carrier transport is improved by the existence of the surface states. We are fairly convinced of the beneficial contributions from factors 1 and 3, but we are still uncertain about 2.

Although the UV effect can result in remarkable increases in efficiency (up to 45-fold) and is completely reproducible, it also involves many of the most difficult and least understood aspects of DSSCs and of semiconductor photoelectrochemistry. It is a major and ongoing challenge to understand this effect in detail. The key experiments for the future may involve time-resolved measurements of the injection and recombination rates and measurements of transport properties.

Acknowledgment. We thank Dr. Kurt Benkstein for assistance with sealing the dye-sensitized solar cells and thank one of the reviewers for extensive comments on the manuscript. We are grateful to the U.S. DOE, Office of Science, Division of Basic Energy Sciences, Chemical Sciences Division, for supporting this research.

References and Notes

(1) O'Regan, B.; Grätzel, M. *Nature* **1991**, *353*, 737−740.
(2) Hagfeldt, A.; Grätzel, M. *Acc. Chem. Res.* **2000**, *33*, 269−277.
(3) Gregg, B. A. In *Semiconductor Photochemistry and Photophysics*; Schanze, K. S., Ramamurthy, V., Ed.; Marcel Dekker: New York, 2003; Vol. 10, pp 51−88.
(4) Gerischer, H. In *Photoelectrochemistry, Photocatalysis and Photoreactors*; Schiavello, M., Ed.; D. Reidel: Dordrecht, Germany, 1985; pp 39−106.
(5) Nozik, A. J.; Memming, R. *J. Phys. Chem.* **1996**, *100*, 13061−13078.
(6) Fahrenbruch, A. L.; Bube, R. H. *Fundamentals of Solar Cells. Photovoltaic Solar Energy Conversion*; Academic Press: New York, 1983.
(7) Parkinson, B. A. *Langmuir* **1988**, *4*, 967−976.
(8) Parkinson, B. A.; Spitler, M. T. *Electrochim. Acta* **1992**, *37*, 943−948.
(9) Wang, H.; He, J.; Boschloo, G.; Lindström, H.; Hagfeldt, A.; Lindquist, S.-E. *J. Phys. Chem. B* **2001**, *105*, 2529−2533.
(10) Hagfeldt, A.; Grätzel, M. *Chem. Rev.* **1995**, *95*, 49−68.
(11) Schlichthörl, G.; Huang, S. Y.; Sprague, J.; Frank, A. J. *J. Phys. Chem. B* **1997**, *101*, 8141−8155.
(12) Solbrand, A.; Lindström, H.; Rensmo, H.; Hagfeldt, A.; Lindquist, S.-E.; Södergren, S. *J. Phys. Chem. B* **1997**, *101*, 2514−2518.
(13) van de Lagemaat, J.; Frank, A. J. *J. Phys. Chem. B* **2000**, *104*, 4292−4294.
(14) de Jongh, P. E.; Vanmaekelbergh, D. *J. Phys. Chem. B* **1997**, *101*, 2716−2722.
(15) Dloczik, L.; Ileperuma, O.; Lauermann, I.; Peter, L. M.; Ponomarev, E. A.; Redmond, G.; Shaw, N. J.; Uhlendorf, I. *J. Phys. Chem. B* **1997**, *101*, 10281−10289.
(16) Boschloo, G. K.; Goossens, A.; Schoonman, J. *J. Electroanal. Chem.* **1997**, *428*, 25−32.
(17) Kay, A.; Humphry-Baker, R.; Grätzel, M. *J. Phys. Chem.* **1994**, *98*, 952−959.
(18) Schwarzburg, K.; Willig, W. *Appl. Phys. Lett.* **1991**, *58*, 2520−2522.
(19) Nelson, J. *Phys. Rev. B* **1999**, *59*, 15374−15380.
(20) Könnenkamp, R.; Henninger, R.; Hoyer, P. *J. Phys. Chem.* **1993**, *97*, 7328.
(21) Haque, S. A.; Tachibana, Y.; Klug, D. R.; Durrant, J. R. *J. Phys. Chem. B* **1998**, *102*, 1745−1749.
(22) Haque, S. A.; Tachibana, Y.; Willis, R. L.; Moser, J. E.; Grätzel, M.; Klug, D. R.; Durrant, J. R. *J. Phys. Chem. B* **2000**, *104*, 538−547.
(23) Huber, R.; Spörlein, S.; Moser, J. E.; Grätzel, M.; Wachtveitl, J. *J. Phys. Chem. B* **2000**, *104*, 8995−9003.
(24) Tachibana, Y.; Haque, S. A.; Mercer, I. P.; Moser, J. E.; Klug, D. R.; Durrant, J. R. *J. Phys. Chem. B* **2001**, *105*, 7424−7431.
(25) Ferrere, S.; Gregg, B. A. *J. Phys. Chem. B* **2001**, *105*, 7602−7605.

(26) Ferrere, S.; Gregg, B. A. *New J. Chem.* **2002**, *26*, 1155−1160.
(27) Zaban, A.; Ferrere, S.; Gregg, B. A. *J. Phys. Chem. B* **1998**, *102*, 452−460.
(28) Nazeeruddin, M. K.; Kay, A.; Rodicio, I.; Humphry-Baker, R.; Müller, E.; Liska, P.; Vlachopoulos, N.; Grätzel, M. *J. Am. Chem. Soc.* **1993**, *115*, 6382−6390.
(29) Zaban, A.; Ferrere, S.; Sprague, J.; Gregg, B. A. *J. Phys. Chem. B* **1997**, *101*, 55−57.
(30) Ferrere, S.; Gregg, B. A. *J. Am. Chem. Soc.* **1998**, *120*, 843−844.
(31) Gregg, B. A.; Pichot, F.; Ferrere, S.; Fields, C. L. *J. Phys. Chem. B* **2001**, *105*, 1422−1429.
(32) Oskam, G.; Bergeron, B. V.; Meyer, G. J.; Searson, P. C. *J. Phys. Chem. B.* **2001**, *105*, 6867−6873.
(33) Nusbaumer, H.; Moser, J.-E.; Zakeeruddin, S. M.; Nazeeruddin, M. K.; Grätzel, M. *J. Phys. Chem. B* **2001**, *105*, 10461−10464.
(34) Kuciauskas, D.; Freund, M. S.; Gray, H. B.; Winkler, J. R.; Lewis, N. S. *J. Phys. Chem. B* **2001**, *105*, 392−403.
(35) O'Regan, B.; Schwartz, D. T. *Chem. Mater.* **1998**, *10*, 1501−1509.
(36) Fardi, H. Z.; Winston, D. W.; Hayes, R. E.; Hanna, M. C. *IEEE Trans. Electron. Dev.* **2000**, *47*, 915−921.
(37) Gregg, B. A.; Hanna, M. C. *J. Appl. Phys.* **2003**, *in press.*
(38) Bard, A. J.; Faulkner, L. R. *Electrochemical Methods*; Wiley & Sons: New York, 1980.
(39) Marcus, R. A. *J. Chem. Phys.* **1965**, *43*, 679−701.
(40) Dittrich, T.; Beer, P.; Koch, F.; Weidmann, J.; Lauermann, I. *Appl. Phys. Lett.* **1998**, *73*, 1901−1903.
(41) Pichot, F.; Gregg, B. A. *J. Phys. Chem. B* **2000**, *104*, 6−10.
(42) Schwarzburg, K.; Willig, F. *J. Phys. Chem. B* **1999**, *103*, 5743−5746.
(43) Zaban, A.; Meier, A.; Gregg, B. A. *J. Phys. Chem. B* **1997**, *101*, 7985−7990.
(44) Rothenberger, G.; Fitzmaurice, D.; Grätzel, M. *J. Phys. Chem.* **1992**, *96*, 5983−5986.
(45) Street, R. A. *Hydrogenated Amorphous Silicon*; Cambridge University Press: Cambridge, U.K., 1991; p 417.
(46) Halls, J. J. M.; Walsh, C. A.; Greenham, N. C.; Marseglia, E. A.; Friend, R. H.; Moratti, S. C.; Holmes, A. B. *Nature* **1995**, *376*, 498−500.
(47) Kraabel, B.; McBranch, D.; Sariciftci, N. S.; Moses, D.; Heeger, A. J. *Phys. Rev. B* **1994**, *50*, 18543−18552.
(48) Shaheen, S. E.; Brabec, C. J.; Sariciftci, N. S.; Padinger, F.; Fromherz, T. *Appl. Phys. Lett.* **2001**, *78*, 841−843.
(49) Huang, S. Y.; Schlichthörl, G.; Nozik, A. J.; Grätzel, M.; Frank, A. J. *J. Phys. Chem. B* **1997**, *101*, 2576−2582.
(50) Wang, R.; Hashimoto, K.; Fujishima, A.; Chikuni, M.; Kojima, E.; Kitamura, A.; Shimohigoshi, M.; Watanabe, T. *Adv. Mater.* **1998**, *10*, 135−138.
(51) Hagfeldt, A.; Björksten, U.; Grätzel, M. *J. Phys. Chem.* **1996**, *100*, 8045−8048.